

Ruled surface underlying KcsA potassium channels

Zhenwei Yao and Monica Olvera de la Cruz*

Cite this: *Soft Matter*, 2014, 10, 540

Received 9th October 2013
Accepted 19th November 2013

DOI: 10.1039/c3sm52612g

www.rsc.org/softmatter

Recent experiments have revealed that the opening and closing of the channel is controlled by concertedly rotating and tilting the ends of the alpha-helices in the KcsA ion channels. We recognize these transmembrane alpha-helices as the generating lines of the ruled surface: the hyperboloid of one sheet. The twist-to-shrink feature of the hyperboloid is adopted by KcsA channels in gating the pore as observed in experiments. Our model may shed light on understanding nature's design principles of ion channels. And the conclusions drawn from this study have implications for the design of artificial channels.

Ion channels are pore-forming proteins across the plasma membranes of cells that regulate the ions passage, a crucial process in cell biology.^{1,2} Specifically, potassium ion channels represent an important class of ion channels and they are responsible for the stabilization of the membrane potential.¹ Central to this function is the ability of such channels to control the transmembrane ion flux *via* the gating mechanism, to open and close the channel pore. Due to their functions in regulating the membrane potential, potassium channels constitute potential drug targets for the treatment of diverse disease processes and offer tremendous opportunities for developing new drugs.³ The understanding of the structure–function relationship behind the gating mechanism of ion channels could vastly improve the process of high throughput screening of ion-channel targeted drugs. And it is also of biomimetic significance for the design of artificial channels which have extensive applications ranging from biosensors, water purification to medical treatment.^{4,5} Extensive research on the structure of the bacterial potassium-ion channel KcsA makes it an ideal system to explore the relationship between the gating mechanism and the structure.^{6–8}

The KcsA potassium channel has an elegant backbone structure of four-fold symmetry that is decorated by various chemical groups. Its essential components include four identical twisted subunits spanning the membrane, with the wide end of the channel facing the extracellular space as shown in Fig. 1.^{2,6} Each subunit contains two transmembrane (TM) alpha-helices, TM1 and TM2, as well as a third short helix that makes the ion filter. The four TM1 (TM2) helices form the outer (inner) core of the channel; the TM1 helices face the lipid membrane and the TM2 helices face the central pore. In the gating process, the TM helices experience large scale conformational variation that is coupled with the pH-dependent triggers located at the extracellular end of TM2.^{9,10} The concerted global motion of the

inner TM2 helical bundle directly modulates the size of the central channel pore and controls the opening and closing of the channel, while maintaining the structural integrity.^{6,7,10} The Electron Paramagnetic Resonance (EPR) technology reveals that the motions of the TM2 helices can be decomposed into rotation and tilting relative to the symmetry axis of the channel.⁷ And a pivot point near 1/3 of TM2 from its extracellular end is identified in the analysis of the data from the EPR measurement.⁷ In this work, we identify the twisted TM helices supporting the KcsA channel as the generating lines of the ruled surface: the circular hyperboloid of one sheet.¹¹ It is found that the twist-to-shrink mechanism of the hyperboloid has been adopted by the KcsA channels in gating the pore as observed in experiments. The conclusions drawn from this study have implications for the design of artificial channels and nanopores.

We focus on the motion of the inner TM2 helices that is directly related to the gating mechanism. In the geometric analysis of the TM2 helices, they are modeled as straight lines

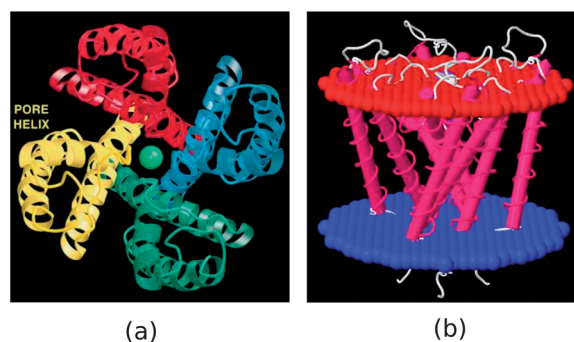


Fig. 1 (a) Stereoview of a ribbon representation of the TM1 and TM2 helices, viewed from the extracellular side. The four subunits are distinguished by color. It is excerpted from ref. 6. Reprinted with permission from AAAS. (b) The side view of the TM1 (the outer four rods) and TM2 (the inner four rods) helices, represented by rods wrapped by spirals, between the membranes.¹²

Department of Materials Science and Engineering, Northwestern University, Evanston, Illinois, 60208-3108, USA. E-mail: m-olvera@northwestern.edu

considering their rigidity during the gating process.^{7,10} The TM2 helices constitute a set of skew lines, which are non-parallel lines with no intersections.¹¹ If one rotates a line L about a skew axis that is not perpendicular to it, the surface of revolution swept out by the line L is a hyperboloid of one sheet.¹¹ The straight line L is the generating line of a ruled surface, which is defined to be the trajectory of moving a straight line in space.¹¹ The TM2 helices are recognized as the generating lines that uniquely define a one-sheeted hyperboloid [see Fig. 1]. Fig. 2 shows some typical ruled surfaces, where (b) and (c) are one-sheeted hyperboloids of different aspect ratios. A hyperboloid of one sheet may also be generated by rotating a hyperbola about the perpendicular bisector to the line between the foci. Note that any three of the four TM2 bundles are not parallel to any plane and also not to each other, so they are excluded from being the generating lines of a hyperbolic paraboloid, a saddle-like ruled surface without rotational symmetry.¹¹ Ruled surfaces are seen in architectures at a length scale of 10 m; now it is interesting to note that they are also involved in biological design at a length scale of 10 Å.¹³

The twist-to-shrink feature of a one-sheeted hyperboloid can nicely fulfill the function of gating an ion channel, as will be illustrated below. Starting from a cylinder composed of rigid rods [Fig. 2(a)], by twisting the two boundary circles, the shape evolves in hyperboloids of varying aspect ratios [Fig. 2(b) and (c)], and finally reaches a double cone structure [Fig. 2(d)]. It is important to notice that for an arbitrary generating line, by simply rotating its end point on the upper boundary circle while fixing the other end, the waist size of the one-sheeted hyperboloid can be significantly changed. Alternatively, one may tune

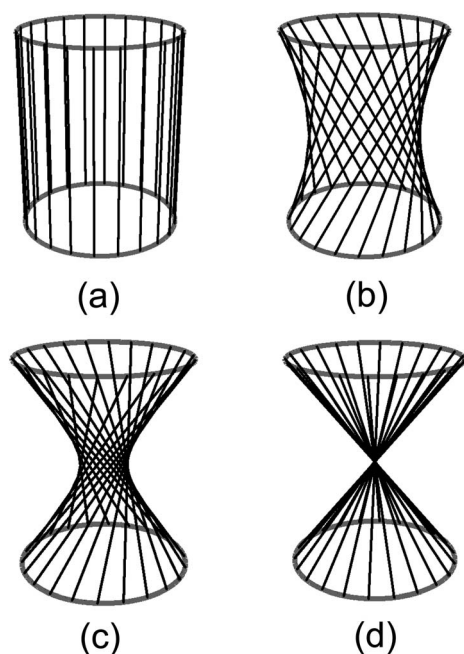


Fig. 2 Straight lines span the two boundary circles. By twisting the upper circle, the surface evolves from cylinder (a), hyperboloid of one sheet (b and c) to the double cone (d).

the radius of the boundary circles to change the waist size of the ruled surface. In both cases, the local motion is converted into a global conformational change. This scheme also enables one to control a small structure (the size of the waist) through manipulating a larger one (the size of the open boundary). The twist-to-shrink feature of the one-sheeted hyperboloid, as demonstrated in Fig. 1, is adopted in KcsA channels in controlling the open and closed states of the pore; both modes of rotating and tilting relative to the symmetry axis of the channel have been observed in experiments using EPR technology.⁷ Biologically, the global conformational change of the channel is triggered by the local motion of the end points of the TM2 helices at the extracellular side that are coupled to the pH-sensitive titratable acidic residues.^{9,10} A similar geometric pattern and gating mechanism is also found in the bacterial mechanosensitive (MS) channel of large conductance MscL, a typical MS channel of five-fold symmetry.^{5,14}

In order to illustrate the variation of the waist size of the ruled surface with the rotating and tilting of generating lines, we consider the geometric configuration in Fig. 3, where the red line represents an arbitrary generating line of the ruled surface spanning the two boundary circles. The shape of the surface changes as the red line experiences rotation (from the straight dashed blue line to the solid red line) and tilting (from the solid red line to the dashed red line). A geometric argument leads to the relationship between the radius of the waist w and the rotating angle θ :

$$w = R \cos \frac{\theta}{2}. \quad (1)$$

It shows that continuous rotation along the same direction (increasing θ), either clockwise or counter-clockwise, leads to shrinking of the waist (decreasing w). The cylinder and double cone are the two limiting cases of a one-sheeted hyperboloid (see Fig. 2). The rotating angle $\theta \in (0, \pi)$ for a one-sheeted hyperboloid. Eqn (1) leads to

$$\frac{dw}{d\theta} = -\frac{R}{2} \sin \frac{\theta}{2}. \quad (2)$$

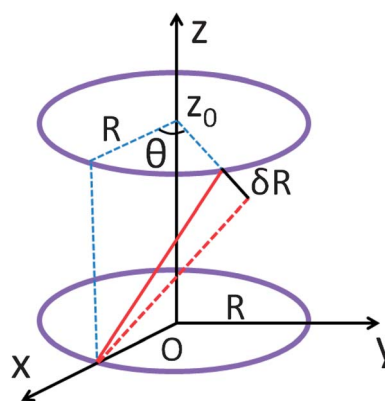


Fig. 3 Schematic plot of a generating line (the solid red line) spanning the two boundary circles, to illustrate how rotating and tilting influence the waist size of the ruled surface.

The absolute value of the RHS of eqn (2) reaches a maximum at $\theta = \pi$. It indicates that when approaching the double cone (θ approaches π), the same amount of rotation brings maximum change of the waist radius. In addition to the rotation mode, the tilting relative to the z -axis is also observed in the KcsA channel.⁷ Now we derive how the radius of the waist w changes by tilting the red line in Fig. 3 away from the z -axis by δR . The radius of the waist is the distance between the tilted line and the z -axis. Given two skew lines passing through the points $\{\mathbf{x}_1, \mathbf{x}_2\}$ and $\{\mathbf{x}_3, \mathbf{x}_4\}$ respectively, their distance is given by¹⁵ $D = \frac{|\mathbf{c} \cdot (\mathbf{a} \times \mathbf{b})|}{|\mathbf{a} \times \mathbf{b}|}$, where $\mathbf{a} = \mathbf{x}_2 - \mathbf{x}_1$, $\mathbf{b} = \mathbf{x}_4 - \mathbf{x}_3$ and $\mathbf{c} = \mathbf{x}_3 - \mathbf{x}_1$. After some calculation, we obtain the increase of the radius of the waist due to the tilting of the generating lines (see Fig. 3):

$$\frac{dw}{dR} = \frac{1}{2} \cos \frac{\theta}{2}. \quad (3)$$

Since $\theta \in (0, \pi)$ for a one-sheeted hyperboloid, $dw/dR > 0$, indicating that tilting towards the z -axis ($dR < 0$) decreases the radius of the waist. Eqn (2) and (3) describe how the size of the waist changes in rotating and tilting the generating lines. In order to get the magnitude of rotation and tilting for opening a typical ion channel, we insert the following parameters into eqn (2) and (3): $\delta w \sim 1 \text{ \AA}$ (the magnitude of the size of an ion), $R \sim 10 \text{ \AA}$ (the size of an ion channel) and the rotating angle $\theta = \pi/2$. We finally obtain the variation of the rotating angle $\delta\theta \approx 0.3 \text{ rad}$ and the amount of tilting $\delta R \approx 3 \text{ \AA}$, which are reasonably small numbers that are possible to be realized *in vivo* and *in vitro*.

Now we compare the geometric model with experiments where in the gating process the TM2 helices concertedly rotate about 8 degrees and tilt by about 8 degrees with respect to the membrane normal.⁷ The pivot points are located near 1/3 of the length of the TM2 helices from their extracellular ends, arising from complicated interactions among protein residues.⁷ We work in the coordinates in Fig. 4. The radii of the lower and upper boundary circles are $R_1 = \frac{5}{8}R_2$ and $R_2 = 10 \text{ \AA}$, respectively.⁷ The height $z_0 = 40 \text{ \AA}$. Due to the symmetry of the

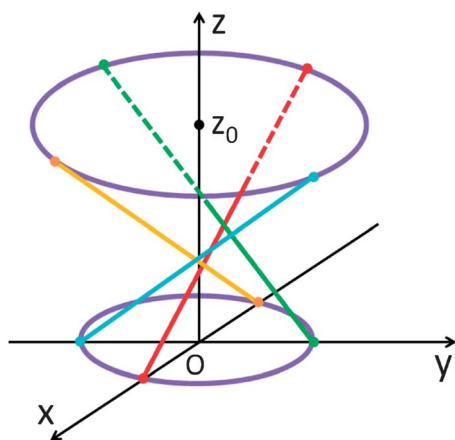


Fig. 4 The schematic plot of the four inner TM2 helices that are represented by straight lines. They are recognized as the generating lines of the one-sheeted hyperboloid (see text for more information).

generating lines, we pick up an arbitrary line, say the blue one, to perform the calculation. In the closed state as in Fig. 4, the coordinates of the two end points of the blue line are $\mathbf{x}_1 = \{0, -R_1, 0\}$ and $\mathbf{x}_2 = \{R_2 \cos(\pi/4), R_2 \sin(\pi/4), z_0\}$. The pivot point \mathbf{x}_{fix} is located at 1/3 of the line near the upper end point, so $\mathbf{x}_{\text{fix}} = \mathbf{x}_1 + \frac{2}{3}(\mathbf{x}_2 - \mathbf{x}_1)$. After tilting and rotating by 8 degrees, the new coordinates of the upper end point are $\mathbf{x}'_2 = \{R'_2 \cos(\pi/4 + \delta\theta_{\text{rot}}), R'_2 \sin(\pi/4 + \delta\theta_{\text{rot}}), z_0\}$, where $R'_2 = R_2 - \frac{1}{3}z_0\delta\theta_{\text{tilt}}$ and $\delta\theta_{\text{rot}} = \delta\theta_{\text{tilt}} = 8 \text{ degrees}$. The increase of the waist size is $2\delta w = 3 \text{ \AA}$, which is comparable with the experimental value of 2 \AA .⁷ This deviation may be attributed to the slight bending of the TM2 helices.⁷ Our calculation also shows that the narrowest point of the channel is located at $z_{\text{narrow}} \approx 9.3 \text{ \AA}$ instead of the $z = 0$ plane, which qualitatively agrees with the experimental value of $z_{\text{narrow}} \approx 12 \text{ \AA}$.⁷

This study shows that the organization of the transmembrane proteins is nicely compatible with their gating mechanism by following the shape of the one-sheeted hyperboloid. Concerted local rotating and tilting of one end of the TM helices are shown to be able to tune the waist size of the channel that is crucial for the gating of the pore. The twist-to-shrink feature of the ruled surface of the one-sheeted hyperboloid may find its application in the design of artificial channels embedded on lipid membranes or bilayer graphenes.¹⁶

Acknowledgements

We thank the support of the Office of the Secretary of Defense under the NSSEFF program award number FA9550-10-1-0167.

References

- 1 B. Hille, *Ionic Channels of Excitable Membranes*, Sinauer associates, Sunderland, MA, 2nd edn, 1984.
- 2 A. Lehninger, D. Nelson and M. Cox, *Lehninger Principles of Biochemistry*, WH Freeman & Co, 1st edn, 2005.
- 3 H. Wulff, N. A. Castle and L. A. Pardo, *Nat. Rev. Drug Discovery*, 2009, **8**, 982–1001.
- 4 T. Fyles, *Chem. Soc. Rev.*, 2007, **36**, 335–347.
- 5 I. Iscla and P. Blount, *Biophys. J.*, 2012, **103**, 169–174.
- 6 D. A. Doyle, J. M. Cabral, R. A. Pfuetzner, A. Kuo, J. M. Gulbis, S. L. Cohen, B. T. Chait and R. MacKinnon, *Science*, 1998, **280**, 69–77.
- 7 Y. Liu, P. Sompornpisut and E. Perozo, *Nat. Struct. Mol. Biol.*, 2001, **8**, 883–887.
- 8 Y. Zhou, J. Morais-Cabral, A. Kaufman and R. MacKinnon, *Nature*, 2001, **414**, 43–48.
- 9 L. Cuello, J. Romero, D. Cortes and E. Perozo, *Biochemistry*, 1998, **37**, 3229–3236.
- 10 Y. Shen, Y. Kong and J. Ma, *Proc. Natl. Acad. Sci. U. S. A.*, 2002, **99**, 1949.
- 11 D. Hilbert and S. Cohn-Vossen, *Geometry and the Imagination*, American Mathematical Society, 1999.
- 12 <http://www.bioinformatics.org>.

- 13 S. Flöry and H. Pottmann, *Proceedings of the Conference of the Association for Computer Aided Design in Architecture (ACADIA)*, 2010.
- 14 M. Faris, D. Lacoste, J. Pécréaux, J. Joanny, J. Prost and P. Bassereau, *Phys. Rev. Lett.*, 2009, **102**, 38102.
- 15 W. Gellert, *The VNR concise encyclopedia of mathematics*, Van Nostrand Reinhold, 1989.
- 16 Z. Sun, A.-R. O. Raji, Y. Zhu, C. Xiang, Z. Yan, C. Kittrell, E. Samuel and J. M. Tour, *ACS Nano*, 2012, **6**, 9790–9796.